Conformational Analysis of Poly(methylene-1,3-cyclopentane) and Chain Conformation in the Crystalline Phase

Odda Ruiz de Ballesteros, Luigi Cavallo, Finizia Auriemma,* and Gaetano Guerra

Dipartimento di Chimica, Università di Napoli, Via Mezzocannone 4, I-80134 Napoli, Italy

Received February 14, 1995; Revised Manuscript Received May 23, 1995®

ABSTRACT: A conformational analysis for poly(methylene-1,3-cyclopentane) (PMCP) for different microstructures is presented. Independently of the microstructure of PMCP, extended conformations suitable for the disordered crystalline phase are geometrically and energetically feasible. However, strong restrictions to the conformational freedom, both of the rings and of the backbone, are required. The similarity between the experimental diffraction profiles of a PMCP sample and the Fourier transform calculations for isolated PMCP extended chains confirms that the crystalline phase of PMCP consists of parallel extended chains (configurationally and conformationally disordered) with a pseudohexagonal arrangement of the chain axes but with a nearly complete intermolecular rotational and translational disorder along the chain axes. The large increases of the entropy of melting with all the examined kinds of configurational order (*cis* or *trans* or isotactic) would be due to the related higher conformational order in the disordered crystalline phase.

Introduction

Cyclopolymerization of 1,5-hexadiene to poly(methylene-1,3-cyclopentane) (PMCP) was first reported by Marvel and co-workers[1,2] and further investigated by Makowski[3] and Cheng[4] by heterogeneous catalysts and more recently by Resconi and Waymouth[5,6] by homogeneous catalysts. For PMCP four microstructures of maximum order are possible (Chart 1).[7] Depending on the catalytic system used,[8] polymers with different kinds of microstructure have been obtained: random-atactic,[5] random-isotactic,[3] *cis*-atactic,[5,6] *trans*-atactic,[5,6] and *trans*-isotactic.[9,10]

According to a recent X-ray diffraction study by some of us,[11] independently of the polymer microstructure, a common disordered crystalline form presenting a long-range positional order (pseudohexagonal) for the axes of configurationally and conformationally disordered chains is observed. Chain repetition periods close to 4.8 Å indicate the presence of extended chain conformations.

A conformational analysis performed in the early sixties[3] suggested that this identity period can be accounted for only by repeating units presenting a *cis* configuration of the cyclopentane ring in a given conformation (envelope). This, of course, contradicts the recent experimental observation of similar crystalline structures with extended chain conformations independently of the microstructure.

In this paper a conformational analysis for PMCP of different microstructures is presented. The main interest is in the investigation of the energetical and geometrical feasibility of extended chains for the different microstructures of PMCP. Fourier transform calculations for isolated chains with suitable geometrical and energetical requirements are also presented for a comparison with the previously reported X-ray diffraction data.[11]

The conformational analysis is first applied to 1,3-dimethylcyclopentane for the two possible configurations (*cis* or *trans*) of the ring. Then the analysis is extended to a dimeric unit of PMCP for the four configurations (*cis*-diisotactic, *cis*-disyndiotactic, *trans*-diisotactic, *trans*-disyndiotactic) corresponding to the polymer microstructures of maximum order. Finally, the analysis is extended to long PMCP chains both configurationally ordered and disordered.

Chart 1

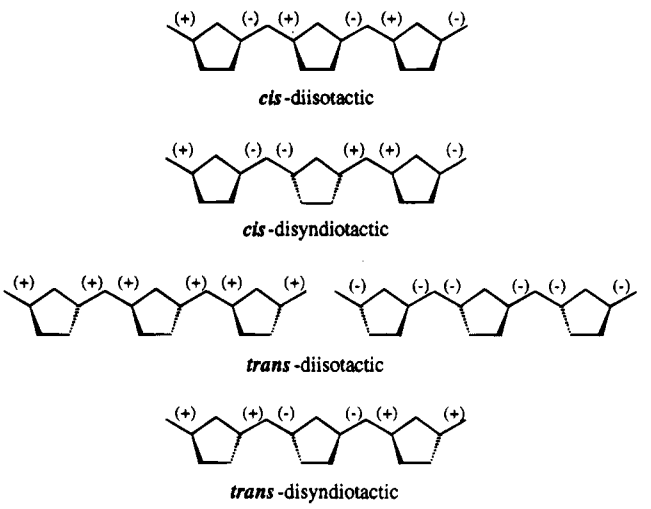

A qualitative comparison of the conformational freedom of the isolated PMCP chains in the crystalline phase and in the melt for different microstructures is also presented. The aim is to find possible insights for the understanding of the large variations with the microstructure observed for the melting entropy.[11]

Calculation Methods

Conformational Analysis. The conformational analysis has been performed keeping, for the sake of simplicity, all the bond distances fixed at 1.54 Å. To simplify the calculations, the hydrogen atoms were not explicitly considered and the CH, CH_2, and CH_3 groups have been treated as identical spherical domains. The conformational energy, according to our model, is thus given by the sum of the terms

$$E = E_{ben} + E_{tor} + E_{nb}$$

where E_{ben} is the sum of the energy contributions

® Abstract published in *Advance ACS Abstracts,* September 1, 1995.

0024-9297/95/2228-7355$09.00/0

associated with the deformation of the bond angles τ from the equilibrium value τ_0, with terms of the kind

$$E_{ben} = (K_{ben}/2)(\tau - \tau_0)^2$$

with $K_{ben} = 44.0$ kcal/(mol deg^2) and $\tau_0 = 109.47°$;[12] E_{tor} is the sum of the energy contributions associated with torsion angles θ, evaluated by terms of the kind

$$E_{tor} = (K_{tor}/2)(1 + \cos n\,\theta)$$

with barrier height $K_{tor} = 2.8$ kcal/mol and periodicity $n = 3$;[12] E_{nb} is the sum of the nonbonded energy contributions due to interactions between atoms separated by more than two bonds, evaluated by terms of the kind

$$E_{nb} = (Ar^{-12} - Br^{-6}) - (Ar_0^{-12} - Br_0^{-6}) \qquad \text{for } r < r_0$$

where r is the interatomic distance for any given couple of nonbonded atoms. In order to avoid negative contributions to the energy, as discussed in ref 13, E_{nb} is fixed equal to zero for $r \geq r_0$, where r_0 is the interatomic distance corresponding to the minimum of E_{nb}. The repulsive and attractive constants A (0.2329×10^7 kcal Å^{12}/mol) and B (0.1137×10^4 kcal Å^6/mol) and r_0 (4.0 Å) are those proposed by Flory in ref 14 for CH_3. Substantially identical results are obtained by choosing for the methine groups the parameters proposed by Flory for C_{sp^3} ($A_{CH-CH} = 0.398 \times 10^6$ kcal Å^{12}/mol, $B_{CH-CH} = 0.366 \times 10^3$ kcal Å^6/mol, $r_0 = 3.6$ Å; $A_{CH-CH_2} = A_{CH-CH_3} = 0.968 \times 10^6$ kcal Å^{12}/mol, $B_{CH-CH_2} = B_{CH-CH_3} = 0.643 \times 10^3$ kcal Å^6/mol, $r_0 = 3.8$ Å).

For the PMCP configurationally ordered and disordered chains the energy minimizations have been performed on chain stretches of 10 monomeric units, including all the interactions. The energies per monomeric unit are then obtained by dividing by 10. The BFGS[15] minimization method was used to find the lowest conformational energy.

Fourier Transform Calculations. Fourier transform calculations have been performed on isolated chain models obtained by regular or irregular sequences of monomeric units in different conformations.

The Fourier transform of isolated chains can be advantageously compared to the diffracted intensity far from the equator, when there is a low degree of rotational (around the chain axis) and translational (along the chain axis) order between adjacent parallel chains. Near the equator the comparison is, instead, less significant, since interferences between adjacent chains should also be taken into account.

The X-ray diffraction intensity by fibers is conveniently calculated as a function of the reciprocal space cylindrical coordinates ξ, Φ, and ζ, as

$$I(\xi,\Phi,\zeta) = F(\xi,\Phi,\zeta)F^*(\xi,\Phi,\zeta) \qquad \text{(I)}$$

where $F(\xi,\Phi,\zeta)$ is the structure factor and the * denotes the complex conjugate. For the calculation of the diffraction intensity by an isolated chain cylindrically averaged over the reciprocal coordinate Φ, we have applied the treatment reported by Tadokoro in ref 16 for the calculation of the molecular structure factor of nonhelical molecules.

Let r_a (r_b), ϕ_a (ϕ_b), and z_a (z_b) be the cylindrical coordinates of the a-th (b-th) atom and n the total number of atoms in the structural model. $I(\xi,\Phi,\zeta)$ is evaluated as

$$I(\xi,\Phi,\zeta) = \sum\sum f_a f_b \exp\{-2\pi i[\xi r_a \cos(\phi_a - \Phi) - \xi r_b \cos(\phi_b - \Phi) + \zeta(z_a - z_b)]\} \qquad \text{(II)}$$

where f_a (f_b) are the atomic scattering factors for the a-th (b-th) atoms. The cylindrically averaged diffraction intensity is evaluated by integration of eq II over Φ. Equation II contains the sum of exponential terms, which after some algebraic transformation, become

$$\exp\{-2\pi i\xi[r_a \cos(\phi_a - \Phi) - r_b \cos(\phi_b - \Phi)]\} = \exp\{-2\pi i\xi[(r_a \cos\phi_a - r_b \cos\phi_b)\cos\Phi + (r_a \sin\phi_a - r_b \sin\phi_b)\sin\Phi]\} \qquad \text{(III)}$$

With introduction of auxiliary variables r_{ab}, representing the distance in the xy plane between the a-th and b-th atoms, and ϕ_{ab}, the angle between the vector r_{ab} and the x axis, the exponential term on the right side of eq III can be rewritten as

$$\exp\{-2\pi i\xi[(r_a \cos\phi_a - r_b \cos\phi_b)\cos\Phi + (r_a \sin\phi_a - r_b \sin\phi_b)\sin\Phi]\} = \exp[2\pi i\xi r_{ab}\cos(\phi_{ab} - \Phi)] \qquad \text{(IV)}$$

Hence, the integral of eq II over Φ becomes the sum of integrals of the kind

$$\int \exp[2\pi i\xi r_{ab}\cos(\phi_{ab} - \Phi)]\,d\Phi \qquad \text{(V)}$$

multiplied by terms which do not depend on Φ. Integrals of this kind have as solution 2π multiplied by the zero-order Bessel function with argument $2\pi\xi r_{ab}$, $J_0(2\pi\xi r_{ab})$.

The resulting formula (dividing the integral by 2π) is

$$I(\xi,\Phi,\zeta) = \sum\sum f_a f_b J_0(2\pi\xi r_{ab}) \exp[-2\pi i\zeta(z_a - z_b)] \qquad \text{(VI)}$$

For the sake of simplicity no thermal factor was included.

The reported Fourier transform calculations refer to models including 10 monomeric units. This choice makes the broadness of the meridional peak on the first layer line (independent of the configurational disorder) similar to the observed one (half-height width close to 1°).

Results and Discussion

A. Conformational Analysis. Conformational Analysis of Cyclopentane. We started the conformational analysis studies with the parent compound cyclopentane. It is well known that the potential energy surface of cyclopentane is very flat and the ring freely pseudorotates between the half-chair and envelope forms (having C_2 and C_s symmetry, respectively (see Chart 2)).[17-23] To describe the pseudorotation phenomenon, the following expression for the torsional angles σ_k was proposed[18-24]

$$\sigma_k = \sigma_0 \cos(4\pi Bk/5 + P) \qquad k = 1, 2, 3, 4, 5$$

where σ_0 is the maximum value of the torsional angle, B the conversion factor from radians to degrees, and P the phase angle of puckering. Deformations described by P values equal to 0°, 36°, 72°, ..., correspond to half-chair forms; those described by values of 18°, 54°, 90°,

Chart 2

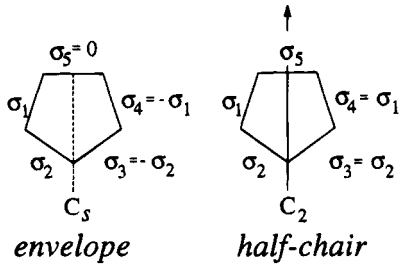

... correspond to envelope forms. As P varies from 0 to 360°, the structure goes through all possible C_2 and C_s forms.

The absolute values of the dihedral angles of cyclopentane corresponding to the energy minima are for the C_s symmetry $|\sigma_1| = |\sigma_4| = 29.7°$, $|\sigma_2| = |\sigma_3| = 45.3°$, and $|\sigma_5| = 0°$ and for the C_2 symmetry $|\sigma_1| = |\sigma_4| = 37.2°$, $|\sigma_2| = |\sigma_3|$ 15.3°, and $|\sigma_5|$ 46.7°. These results compare well with some literature results.[17,19,21]

The energy difference between the C_s and C_2 structures is negligible (<50 cal/mol), and the energy profile along the pseudorotational path connecting the C_s and the C_2 conformations, obtained by energy minimization of several conformations of no symmetry, is practically flat.

Conformational Analysis of 1,3-Dimethylcyclopentane. At variance with the case of the parent compound, for the disubstituted cyclopentane the energy barriers to the pseudorotation are high, and large energy differences are obtained between conformations which are all substantially isoenergetic for cyclopentane.

For the present analysis we use the terminology proposed by Fuchs[25] for 1,3-dichlorocyclopentane. The full pseudorotational circuit (sketched in Figures 1 and 2 of ref 25) presents 5 half-chair conformations (enantiomeric pairs) and 6 envelope conformations (including 4 enantiomeric pairs) for the *cis* isomer and 6 half-chair conformations and 5 envelope conformations for the *trans* isomer. All the conformations are labeled by roman numerals, and an attached star indicates the enantiomeric conformation.

In the geometrical and energetical calculations the absolute values of the dihedral angles, relative to the cycles, are maintained fixed to those corresponding to the energy minimization for cyclopentane (reported in the previous section).

The calculated energy, optimized with respect to the bending of the two methyl groups, and the distance d between the carbon atoms of the two methyl substituents for the *cis* and *trans* isomers are reported versus the phase angle (P) in parts A and B of Figure 1, respectively. In the figure the ring conformations are also indicated following the nomenclature of Fuchs.

It is apparent that broad energy minima are present for both isomers, in particular centered around conformation XI for the *cis* isomer and around conformation I for the *trans* isomer.

The conformations included in these broad energy minima are also those for which the distance d is in the range 4.8–5.0 Å. It is hence reasonable to expect that sequences of monomer units in these conformations, if nearly perfectly aligned, can produce the chains with periodicity along c of nearly 4.8 Å, which are present in the crystalline phase of PMCP.[11] The conformations corresponding to the structures IX, X, XI, X*, and IX* for the *cis* isomer and I, II, and III for the *trans* isomer are sketched in parts A and B of Figure 2, respectively.

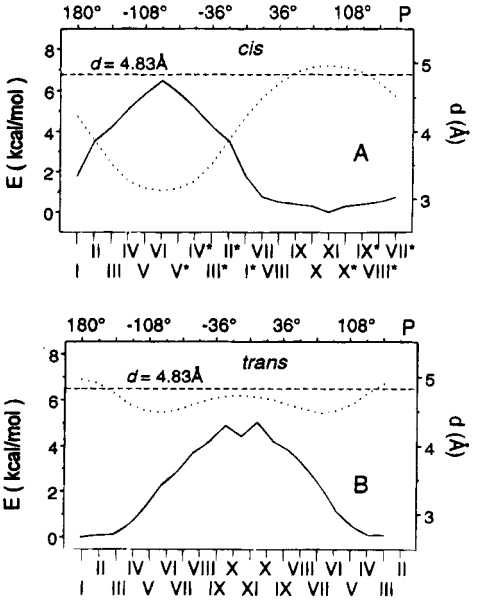

Figure 1. Energy profile (solid line) and distance (d) between the carbon atoms of the two methyl substituents (dotted line) for the pseudorotation circuit of (A) *cis*-1,3-dimethylcyclopentane and (B) *trans*-1,3-dimethylcyclopentane. The pseudorotation circuit is indicated by the phase angle P (top scale) and by the nomenclature of Fuchs (bottom scale).

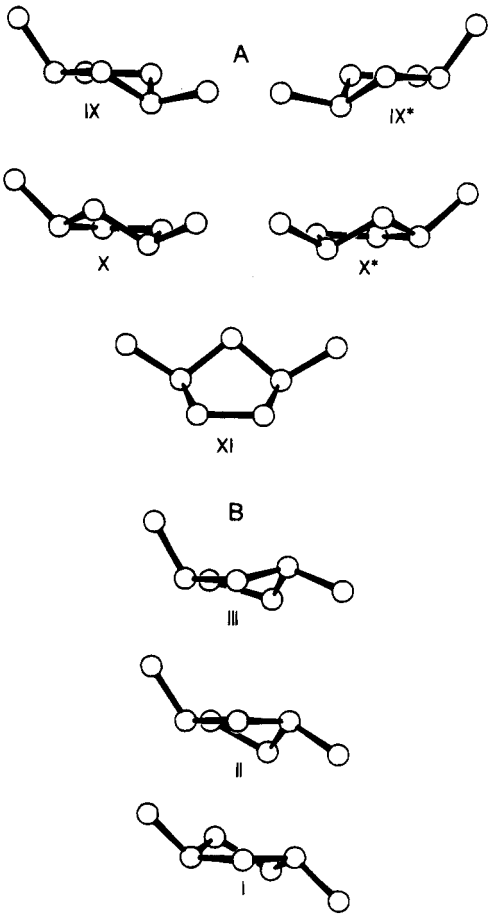

Figure 2. Sketches of some conformations of the two stereoisomers of 1,3-dimethylcyclopentane: (A) conformations IX, X, XI, X*, and IX* of the *cis* isomer; (B) conformations I, II, and III of the *trans* isomer. These conformations are included in the broad energy minima of Figures 1A and 1B, respectively.

Conformational Analysis of a Dimeric Unit of PMCP. A conformational analysis has been performed also for the four microstructures of maximum order for

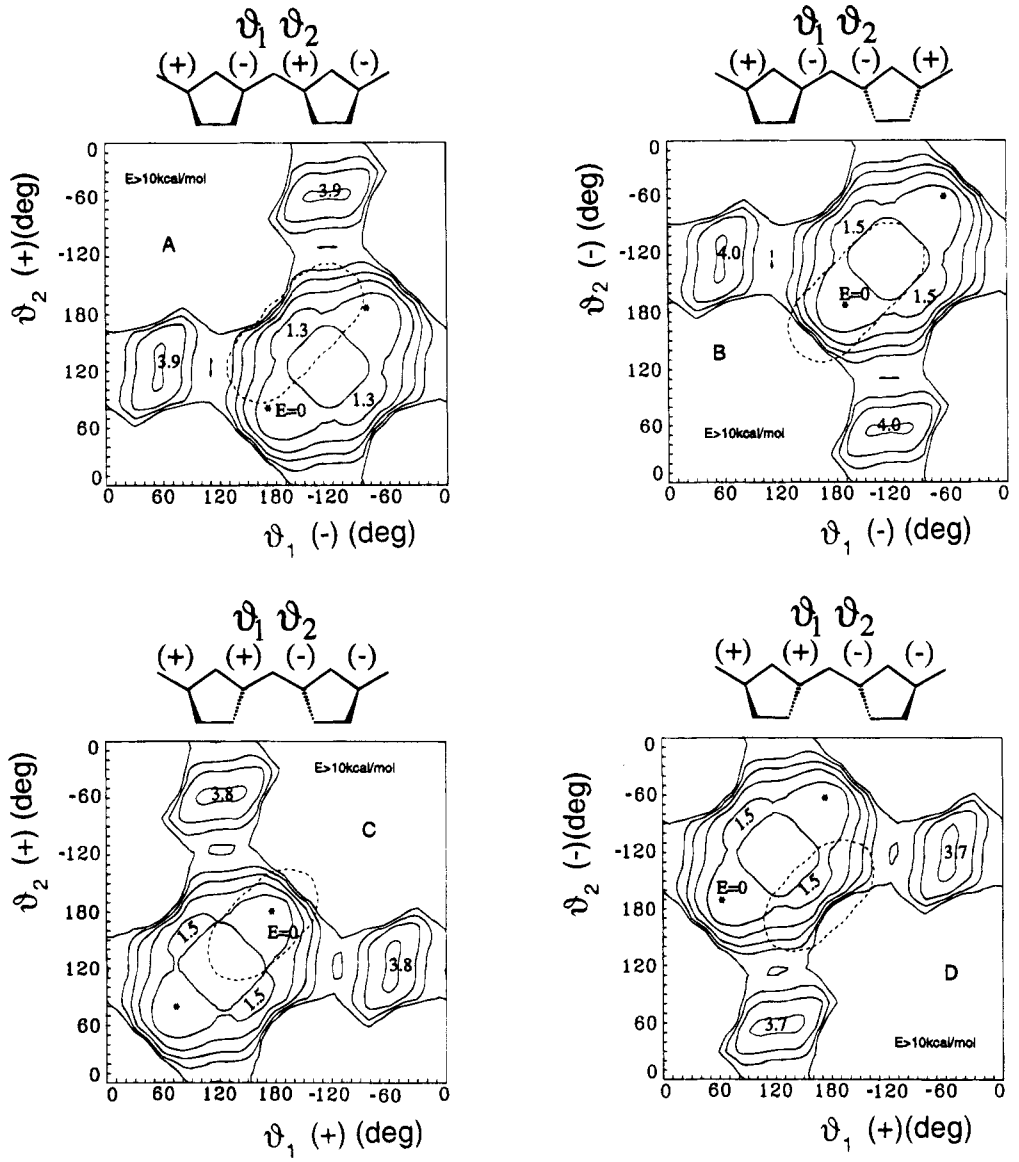

Figure 3. Conformational energy maps $E(\theta_1,\theta_2)$ for the models presenting the four maximum order microstructures: (A) *cis*-diisotactic; (B) *cis*-disyndiotactic; (C) *trans*-diisotactic; (D) *trans*-disyndiotactic. In all cases contour lines with constant conformational energy are at regular intervals of 2 kcal/mol, starting from the absolute minimum; the energy values for the secondary minima are also indicated. The dashed ellipsoids in the maps include the loci of points (θ_1,θ_2) for which the average distance between two consecutive methylene groups (d') is higher than 4.8 Å.

the models shown in Figure 3, corresponding to dimeric units of PMCP. For the sake of simplicity, for the reported energy maps, the bond angle centered on the methylene C atom which connects two rings has been maintained fixed at 112°. For the two cycles conformations XI and I have been always assumed for the *cis* and *trans* rings, respectively. They correspond to conformations geometrically and energetically suitable for the achievement of extended chains, according to the calculations of the previous section. Also in this case the σ values were fixed to the energy minima values for cyclopentane.

For the following discussion, we will attribute a configurational sign[26] to the C−C bonds which connect different rings (see Chart 1). The sequence of the configurational signs is, indicating by a slash the position along the backbone of a cyclopentane ring, (−)(+)/(−)(+) for the *cis*-diisotactic, (−)(−)/(+)(+) for the *cis*-disyndiotactic, (+)(+)/(+)(+) (or the enantiomoprhic (−)(−)/(−)(−)) for the *trans*-diisotactic, and (+)(−)/(−)(+) for the *trans*-disyndiotactic microstructure. Without loss of generality in this paper, we consider for the *trans*-diisotactic microstructure only the (+)(+)/(+)(+) sequence.

The conformational energy maps (per mole of monomeric unit) as a function of the dihedral angles θ_1 and θ_2, scanned every 10°, for the *cis*-diisotactic, *cis*-disyndiotactic, *trans*-diisotactic, and *trans*-disyndiotactic microstructures are shown in parts A−D of Figure 3, respectively. Dashed curves in the maps indicate the loci of points for which the average distance between two consecutive methylene groups d' is equal to 4.8 Å.

It is reasonable to assume that only sequences of dimeric units presenting conformations included in these curves, if nearly perfectly aligned, are geometrically suitable for the formation of the extended chains, which are present in the crystalline phase.

The maps of Figure 3 indicate that geometrically suitable conformations are also energetically suitable for all the microstructures. In particular, for the *cis*-disyndiotactic and *trans*-diisotactic microstructures the dashed curves contain the absolute minimum of energy, while for the *cis*-diisotactic and *trans*-disyndiotactic microstructures the curves contain a secondary mini-

Table 1. Dihedral Angles θ_1, θ_2, θ_1', and θ_2', Bond Angles τ, and Energy E^{ext} Values for the Four Maximum Order Microstructures As Obtained after Energy Minimization under the Geometrical Constraint of a Unit Height of 4.83 Å (Extended Conformations)[a]

microstructures	θ_1	θ_2	θ_1'	θ_2'	τ	E^{ext}
cis-diisotactic	−162	162			111.4	1.5
cis-disyndiotactic	175	175	−175	−175	111.9	0.1
trans-diisotactic	−179	−179			110.6	0.3
trans-disyndiotactic	158	−158	−158	158	111.9	1.5

[a] Angles in degrees and energies in kcal/mol.

mum of energy with an energy content of nearly 1.5 kcal/(mol of monomeric unit) higher.

It is worth noting that the general rule for vinyl polymers[26] that (+) bonds tend to assume G_+ or T conformations while (−) bonds tend to assume G_- or T conformations is confirmed by the energy maps of Figure 3.

Conformational Analysis of PMCP. Energy minimizations for the four microstructures of maximum order of PMCP have been performed under the geometrical constraint that the unit height is 4.83 Å. As energy zero for each calculation, the minimum energy calculated for the same model structures in the absence of this constraint has been assumed.

For the sake of simplicity, only the ring conformations XI and I have been considered for *cis* and *trans* rings, respectively, and also the dihedral angles in the rings (σ) have been maintained fixed to the values listed in the preceding sections.

For the isotactic polymers the conformational repeating unit (CRU) is assumed equal to one monomeric unit; in particular, it is assumed $\theta_1 = -\theta_2$ for the *cis* polymer and $\theta_1 = \theta_2$ for the *trans* polymer (see Chart 1). For the syndiotactic polymers the CRU is assumed equal to two monomeric units. Indicating with θ_1, θ_2, and θ_1', θ_2' the dihedral angles of two consecutive monomeric units, for symmetry reasons it is assumed $\theta_1 = \theta_2 = -\theta_1' = -\theta_2'$ for the *cis* polymer and $\theta_1 = -\theta_2 = -\theta_1' = \theta_2'$ for the *trans* polymer (see Chart 1).

As starting situations for the minimization procedures, the minimum energy conformations, included in the dashed curves in the maps of Figure 3, have been assumed. The dihedral and bond angle values which minimize the energy for the extended conformation of the four microstructures are reported in Table 1, together with the corresponding energy per monomeric unit E^{ext}. These minima correspond to values of θ_1 and θ_2 which are positive or negative according to the configurational sign of the bonds (see Chart 1).

Analogous calculations for the stereoirregular polymers under the constraint that the average length of the projection of the monomeric units along the chain axis is 4.83 Å give E^{ext} values intermediate between the minimum and maximum E^{ext} values of Table 1.

In summary, independently of the microstructure of PMCP, extended conformations suitable for the disordered crystalline structure are easily achieved.

However, it is worth noting that in order to obtain low-energy extended conformations, restrictions to the conformational freedom, both of the rings and of the backbone, are required. In particular, the configuration of the cyclopentane rings (*cis* or *trans*) imposes their conformation (close to XI or to I, respectively) while the local configuration (*cis*-diisotactic, *cis*-disyndiotactic, *trans*-diisotactic, or *trans*-disyndiotactic) imposes locally the values of the dihedral angles along the main chain (not far from those of Table 1).

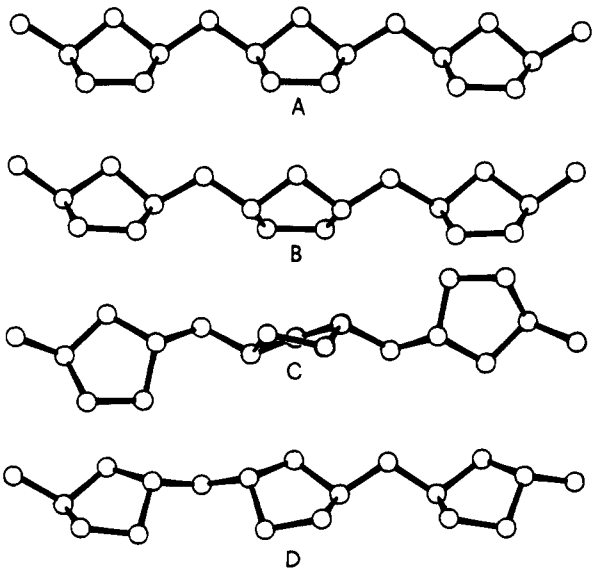

Figure 4. Side views of extended model chains of minimum energy for the microstructures: (A) *cis*-diisotactic; (B) *cis*-disyndiotactic; (C) *trans*-diisotactic; (D) *trans*-disyndiotactic.

Side views of models of extended chains for the four microstructures of maximum order of PMCP are sketched in Figure 4A–D (including three monomeric units). Side views for two random-isotactic extended and energetically feasible chains of PMCP, including 10 monomeric units, are sketched in Figure 5. For the chain of Figure 5A, only one kind of ring conformation (XI for the *cis* and I for the *trans*) is present, while for the chain of Figure 5B further ring conformations (IX, X, X*, and IX* for the *cis* and II and III for the *trans*) are included.

B. Fourier Transform Calculations on Isolated PMCP Chains. The Fourier transform on nonequatorial layer lines for the four microstructures of maximum order of PMCP in the conformations of Table 1 (models shown in Figure 4A–D) is reported in Figure 6A–D. The Fourier transform calculated along the meridian (for $\xi = 0$) for the same models is reported in Figure 7A–D.

For comparison, the experimental diffraction intensities on the layer lines and along the meridian for a random-isotactic PMCP sample after subtraction of background and correction for the LP factor (redrawn from Figure 3B and 4B of ref 11) are shown in Figures 8 and 9, respectively.

The number of monomeric units in the models for the Fourier transform calculations has been fixed equal to 10 in order to reproduce the broadness of the first peak along the meridian.

It is apparent that the Fourier transform of PMCP is scarcely dependent on the microstructure. In fact, the only relevant difference between the plots of Figure 6 is the higher intensity along the meridian on the second layer line for the disyndiotactic structure (*cis* or *trans*) as clearly shown by a comparison of the peaks at $\zeta = 0.42$ Å^{-1} in Figure 7.

A qualitative similarity exists between all the calculated patterns (of Figures 6 and 7) and the experimental diffraction profiles (of Figures 8 and 9). However, significant quantitative differences can be noted for the meridional scans. In particular, the observed peaks for the third and fourth layer lines are much broader (half-height widths $\beta = 2.3°$ and 5.2°, respectively) than the peak of the first layer line ($\beta = 1.9°$), whereas all these peaks present similar broadness in the calculated pat-

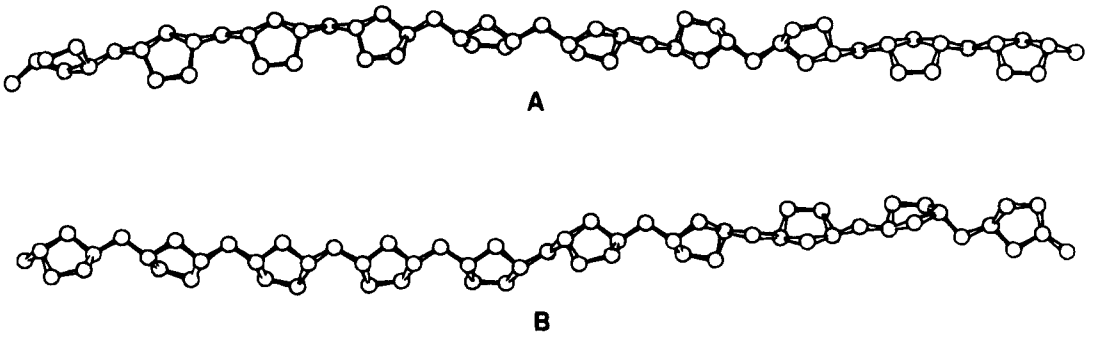

Figure 5. Side views of extended model chains of minimum energy with random-isotactic microstructure including (A) only one kind of ring conformation (XI for the *cis* and I for the *trans*), and (B) several kinds of ring conformations (IX, X, XI, X*, and IX* for the *cis* and I, II, and III for the *trans*.)

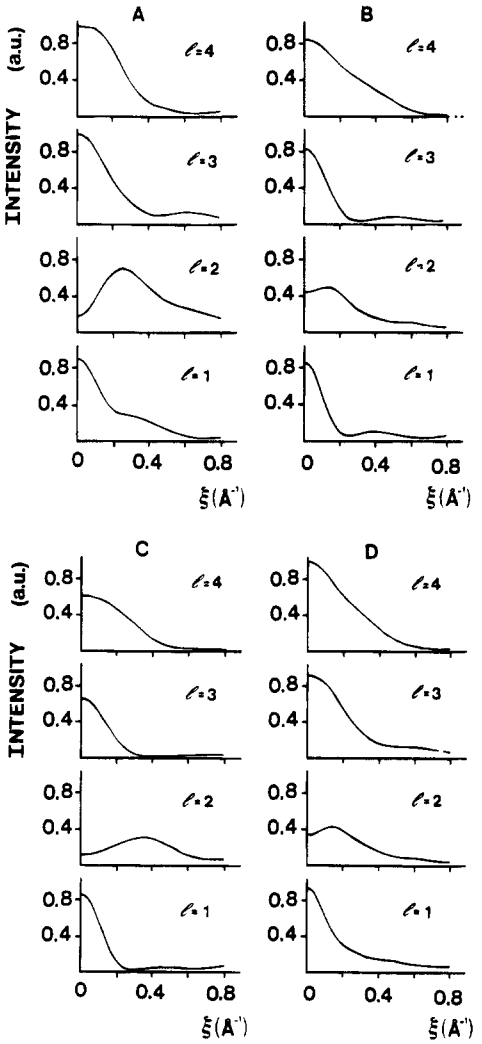

Figure 6. Fourier transform on nonequatorial layer lines (l = 1, 2, 3, 4) for the four microstructures of maximum order in the conformations of Table 1 (models shown in Figures 4A–D): (A) *cis*-diisotactic; (B) *cis*-disyndiotactic; (C) *trans*-diisotactic; (D) *trans*-disyndiotactic.

terns (β close to 1.8°). Correspondingly, the observed meridional peaks on the third and fourth layer lines present a height roughly equal to one-half of the height of the peak on the first layer line, while in all the calculated patterns these peaks present nearly the same heights.

The height of the peak along the meridian on the second layer line is not considered for quantitative evaluations since, as also discussed in ref 11, it is only a broad tail of the maximum located at ξ = 0.22 Å^{-1}

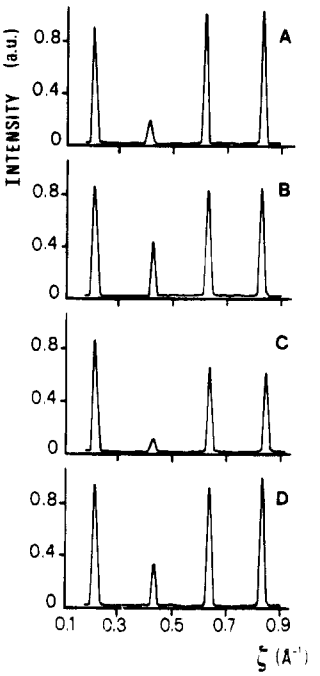

Figure 7. Fourier transform calculated along the meridian (ξ = 0) for the four microstructures of maximum order (same models of Figure 6): (A) *cis*-diisotactic; (B) *cis*-disyndiotactic; (C) *trans*-diisotactic; (D) *trans*-disyndiotactic.

(Figure 8) and hence dependent on the degree of orientation (in particular, the lack of complete orientation of the sample tends to increase the intensity of the experimental peak of the second layer line for ξ = 0, located at ζ = 0.42 Å^{-1} in Figure 9).

The Fourier transform along the layer lines calculated by averaging the results for 10 random-isotactic models analogous to the one shown in Figure 5A, which present only one kind of conformation for the *cis* (XI) and the *trans* (I) rings, is shown in Figure 10. The Fourier transform along the meridian (ξ = 0) for the same models is reported in Figure 11A.

The introduction of stereoirregular sequences in the model chains broadens only slightly the peaks on the third and fourth layer lines (β = 2.0 and 2.3°, respectively).

The Fourier transform along the meridian calculated by averaging the results for 10 random-isotactic models which include also other geometrically and energetically feasible ring conformations is shown in Figure 11B–D.

In particular, a further two (IX and X, with the enantiomers IX* and X*, for the *cis* rings; III and II for the *trans* rings) or three (plus VIII, with the enantiomer VIII*, for the *cis* rings; plus IV for the *trans* rings) or

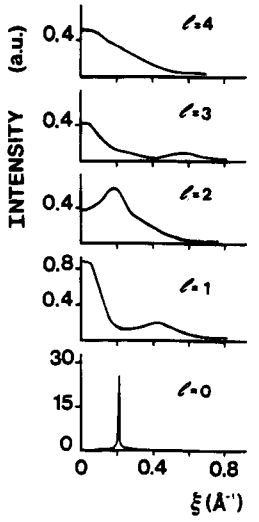

Figure 8. Experimental X-ray diffraction intensity of an oriented random-isotactic PMCP sample for the indicated layer lines l (corresponding to a periodicity of c = 4.83 Å) after subtraction for the background and correction by the Lorentz and polarization factor.

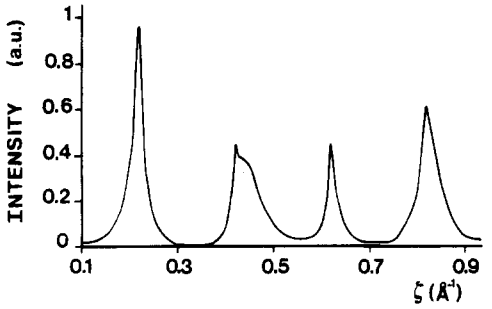

Figure 9. Experimental X-ray diffraction intensity of an oriented random-isotactic PMCP sample along the meridian ($\xi = 0$) after subtraction for the background and correction by the Lorentz and polarization factor.

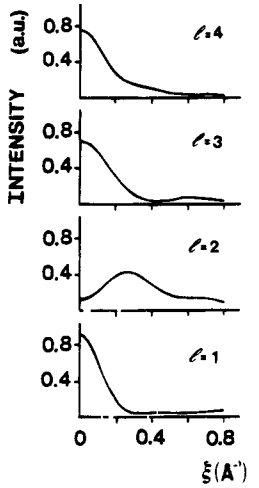

Figure 10. Fourier transform on nonequatorial layer lines calculated by averaging the results for 10 random-isotactic models analogous to the one shown in Figure 5A.

four (plus VII, with the enantiomer VII*, for the *cis* rings; plus V for the *trans* rings) ring conformations are statistically accessible for the calculations of Figure 11B, 11C, and 11D, respectively.

It is apparent that this conformational disorder relative to the rings leaves essentially unaltered the broadness of the meridional peak on the first layer line while, in qualitative agreement with the experimental

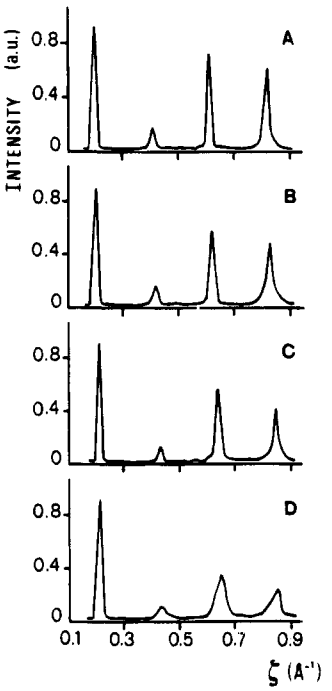

Figure 11. Fourier transform along the meridian calculated by averaging the results of 10 models analogous to those shown in Figure 5. The ring conformations randomly assumed in the models by the *cis* and *trans* rings (with reference to the Fuchs nomenclature used in Figures 1 and 2), also including the possible enantiomeric situations, are (A) XI and I, (B) IX, X, XI and I, II, and III, (C) VIII, IX, X, and XI and I, II, III, and IV, and (D) VII, VIII, IX, X, and XI and I, II, III, IV, and V, respectively.

profile of Figure 8, it makes broader the meridional peaks on the third and fourth layer lines and reduces their heights. In fact, with increasing conformational disorder, the values of β of the third and fourth peaks increase from 2.3 and 2.9° (Figure 11B) to 2.8 and 5.6° (Figure 11D), respectively.

Of course, any disorder along the chain that makes the distribution of the length of the projection of the monomeric units along the chain axis (centered around 4.83 Å) broader makes the layer lines (and hence the meridional peaks) broader, and the broadening is more pronounced for higher layer lines.

It is worth noting that the introduction of the thermal factor along ζ ($\exp(-1/2B_\xi\zeta^2)$) rather than the considered conformational disorder could adjust the intensity ratios among the peaks of different layer lines but would leave equal the broadness along the meridian of all the layer lines.

In summary, the similarity between the experimental diffraction profiles of a PMCP sample and the Fourier transform calculations for isolated PMCP extended chains (with different ordered and disordered microstructures) confirms that the crystalline phase of PMCP consists of parallel extended chains (configurationally and conformationally disordered), with a pseudohexagonal arrangement of the chain axes but with a nearly complete intermolecular rotational and translational disorder between the chains.

The calculations of Figure 11 suggest for the crystalline phase the statistical occurrence of few ring conformations, always included in the broad energy minima calculated for the *cis* and *trans* configurations of 1,3-dimethylcyclopentane (Figure 1).

C. Comments on the Variations of the Melting Entropy of PMCP with the Microstructure. Large

variations of the melting entropy (ΔS_m) with the microstructure have been observed for PMCP.[11] At variance with the melting temperature behavior, which mainly increases with the *cis* stereoregularity of the ring configurations, the entropy of melting tends to increase both with the stereoregularity of the ring configurations and with the tacticity of the polymer. In particular, for the substantially atactic samples, the highest ΔS_m values are reached by the high-*cis* sample, while increases are also observed going from the *trans* to the high-*trans* sample. On the other hand, a comparison of the thermal properties of the two samples having a *cis* content close to 35% shows a much higher ΔS_m (46.02 vs 22.59 kcal/(K mol)) for the polymer with an isotactic stereoregularity between the rings.[11]

It is reasonable to expect that the contribution to the entropy of fusion due to the change of volume that occurs on melting, ΔS_v (which is generally smaller than the entropy change of melting at constant volume $(\Delta S_m)_v$[27]), should be similar for all the PMCP samples, due to similarity of the disordered crystalline structures.

As a consequence, since $\Delta S_m = \Delta S_v + (\Delta S_m)_v$, the large variation in the ΔS_m values for different PMCP microstructures should be related to the term $(\Delta S_m)_v$. This term, for polymer crystals, includes essentially the change in the intramolecular conformational entropy of a polymer chain when passing from the crystalline to the molten amorphous state.

The conformational entropy of the polymer chains in the molten state is expected to be similar for all the PMCP samples having different microstructures. In fact, as shown, for instance, by the energy maps of Figure 3, the conformational freedom of the polymer chain is substantially independent of the chain configuration.

The conformational entropy in the crystalline state is, instead, expected to be dependent on the configurational order. In particular, as specified in a previous section, the configuration of the cyclopentane rings (*cis* or *trans*) imposes their conformation (close to the XI or to the I, respectively) while the relative stereochemistry between the rings (*cis*-diisotactic, *cis*-disyndiotactic, *trans*-diisotactic, or *trans*-disyndiotactic) imposes locally the values of the dihedral angles along the main chain (close to that of Table 1).

Higher configurational order (both inside the rings and between successive rings) generates higher conformational order in the disordered crystalline phase and hence larger changes in the intramolecular conformational entropy in the melting.

Since the other contributions should be essentially independent of the PMCP microstructure, this qualitatively accounts for the observed increases of ΔS_m with all the examined kinds of configurational order (*cis*, *trans*, and isotactic).

Acknowledgment. This work was supported by the Ministero dell'Università e della Ricerca Scientifica e Tecnologica (Italy). X-ray diffraction data were recorded with a Nonius CAD4 automatic diffractometer (Centro Interdipartimentale di Metodologie Chimico Fisiche, University of Naples). We wish to thank Prof. P. Corradini, Prof. R. M. Waymouth, and Dr. L. Resconi for useful discussions.

References and Notes

(1) Marvel, C. S.; Stille, J. K. *J. Am. Chem. Soc.* **1958**, *80*, 1740.
(2) Marvel, C. S.; Garrison, W. E., Jr. *J. Am. Chem. Soc.* **1959**, *81*, 4737.
(3) Makowski, H. S.; Shim, B. K. C.; Wilchinsky, Z. W. *J. Polym. Sci., Part A* **1964**, *2*, 1549.
(4) Cheng, H. N.; Khasat, N. P. *J. Appl. Polym. Sci.* **1988**, *35*, 825.
(5) Resconi, L.; Waymouth, R. M. *J. Am. Chem. Soc.* **1990**, *112*, 4953.
(6) Resconi, L.; Coates, G. W.; Mogstad, A.; Waymouth, R. M. *J. Macromol. Sci.* **1991**, *A28*, 1225.
(7) Farina, M. *Top. Stereochem.* **1987**, *17*, 1.
(8) Cavallo, L.; Guerra, G.; Corradini, P.; Resconi, L.; Waymouth, R. M. *Macromolecules* **1993**, *26*, 260.
(9) Coates, G. W.; Waymouth, R. M. *J. Am. Chem. Soc.* **1991**, *113*, 6270.
(10) Okuda, J. *Angew. Chem., Int. Ed. Engl.* **1992**, *31*, 47.
(11) Ruiz de Ballesteros, O.; Venditto, V.; Auriemma, F.; Guerra, G.; Resconi, L.; Waymouth, R. M.; Mogstad, A. *Macromolecules* **1995**, *28*, 2383.
(12) Suter, U. W.; Flory, P. J. *Macromolecules* **1975**, *8*, 765.
(13) Petraccone, V.; Pirozzi, B.; Frasci, A.; Corradini, P. *Eur. Polym. J.* **1976**, *12*, 323.
(14) Sundararajan, P. R.; Flory, P. J. *J. Am. Chem. Soc.* **1974**, *96*, 5025.
(15) Broyden, C. G. *J. Inst. Math. Appl.* **1970**, *6*, 76. Fletcher, R. *Comput. J.* **1970**, *13*, 317. Goldfarb, D. *Math. Comput.* **1970**, *24*, 23. Shanno, D. F. *Math. Comput.* **1970**, *24*, 647.
(16) Tadokoro, H. *Structure of Crystalline Polymers*; J. Wiley & Sons: New York, 1979.
(17) Kilpatrick, J. E.; Pitzer, K. S.; Spitzer, R. *J. Am. Chem. Soc.* **1947**, *69*, 2483.
(18) Pitzer, K. S.; Donath, W. E. *J. Am. Chem. Soc.* **1959**, *81*, 3213.
(19) Hendrickson, J. B. *J. Am. Chem. Soc.* **1961**, *83*, 4537; and erratum, ibid. **1963**, *85*, 4059.
(20) Lifson, S.; Warshel, A. *J. Chem. Phys.* **1968**, *49*, 5116.
(21) Ferguson, D. M.; Raber, D. J. *J. Am. Chem. Soc.* **1989**, *111*, 4371.
(22) Ferguson, D. M.; Gould, I. R.; Glauser, W. A.; Kollmann, P. A. *J. Comput. Chem.* **1992**, *13*, 535.
(23) Cui, W.; Allinger, N. L. *J. Am. Chem. Soc.* **1993**, *115*, 2943.
(24) Bauman, L. E.; Laane, J. *J. Phys. Chem.* **1988**, *92*, 1040.
(25) Fuchs, B.; Wechsler, P. S. *Tetrahedron* **1977**, *33*, 57.
(26) Corradini, P. In *The Stereochemistry of Macromolecules*; Marcel Dekker: New York, 1968; Vol. 3.
(27) Tonelli, A. E. *J. Chem. Phys.* **1970**, *52*, 4749.

MA9501858